Understanding the 14 February 2024 tornado in Cyprus

Eleni Loulli[*a,b], Silas Michaelides[a], Johannes Bühl[c], Rodanthi-Elisavet Mamouri[a], Argyro Nisantzi[a], Dragoș Ene[a], Patric Seifert[d], Demetris Charalambous[e], Filippos Tymvios[e], Diofantos Hadjimitsis[a,b]
[a]Eratosthenes Centre of Excellence, 82 Franklin Roosevelt, 3012, Lemesos, Cyprus; [b]Cyprus University of Technology, 30 Arch. Kyprianos Str., 3036, Lemesos, Cyprus; [c]Harz University of Applied Sciences, Friedrichstrasse 57-59, 38855, Wernigerode Germany; [d]Leibniz Institute for Tropospheric Research (TROPOS), Permoserstraße 15, 04318, Leipzig, Germany; [e]Department of Meteorology, 28 Nikis, 1086, Nicosia, Cyprus

*eleni.loulli@eratosthenes.org.cy; phone +35725245087; eratosthenes.org.cy

ABSTRACT

On 14 February 2024, Cyprus experienced a significant damaging tornado, characterized by gale force winds, heavy precipitation, and a distinct spiral pattern of thunderstorms. The event caused extensive damage across Limassol district, particularly in Germasogeia suburb. This work examines the potential of using remote sensing observations for the analysis of convective storms associated with tornadic activity. For the analysis of the tornado, we use meteorological radar data from the Department of Meteorology's radar stations in Pafos (PFO) and Larnaca (LCA), in synergy with wind-lidar and disdrometer data from the Cyprus Atmospheric Remote Sensing Observatory (CARO), the latter located in Limassol and at a distance of approximately 10km from the tornado funnel. The analysis involves wind speed data, damage reports and photographic evidence to capture the trail of the tornado. Preliminary results provide evidence of a hook echo and velocity couplets in radar data during the early morning hours on 14 February 2024. During the tornado event, CARO recorded vertical wind speeds of up to 10m/s and an instantaneous rain rate of 80 mm/h.

Keywords: tornado, X-Band radar, disdrometer, wind-lidar, reflectivity, radial velocity

1. INTRODUCTION

Severe thunderstorms and tornadoes occur under extreme weather conditions and can cause serious damages, despite their typically short duration [1]. [2] Fujita (1971) classifies tornadoes based on their wind speed that usually ranges between 20 and 140 $m\,s^{-1}$. Their lifespan ranges from a few seconds to over an hour and their diameter is minimum 200 m [3]. Despite the fact that Central United States experiences the highest number of significant tornados, they are observed and reported globally [4], [5], [6]. The Mediterranean Sea is prone to tornadoes, as its surrounding orographic features such as the Alps, the Pyrenees and the Atlas mountain can trigger vortex development [4]. Cyprus, located in the south-east Mediterranean, experiences tornadoes and water sprouts frequently, especially in the southern coastal regions [6]. Nevertheless, in literature there is limited information about tornadic activity in Cyprus [6], [7]. Water sprouts and tornadoes in Cyprus typically develop south of the island moving from the sea towards the land and dissipating approximately 5 km from the coastline. Water sprouts are most common in January and February, whereas tornadoes generally occur in July and August. This work presents a preliminary approach for understanding a remarkable tornado that occurred in Cyprus in February 2024. To the best of our knowledge this is the first study that combines ground-based weather radar and a Doppler wind lidar and a disdrometer.

On 14 February 2024, early morning hours, Cyprus experienced a damaging tornado, whereas some sources report two tornadoes (see Figure 1). The exact time of the tornado was not officially announced, but based on various newspaper articles, we could conclude that the tornado occurred in the timeframe between 2:30 to to 3:30 a.m. local time (00:30 to 01:30 UTC). The event caused extensive damages across Limassol district, particularly Germasogeia suburb. The storms tore roofs off houses, downed a building crane, and caused significant infrastructural damage. Local officials reported that the damage was massive and unprecedented, with emergency services and maintenance workers responding to the aftermath. Roads within the area were closed due to debris scattered, whereas authorities had claims for damages to over 210 residences and apartments, 17 commercial properties, 25 vehicles and a church. Five homes were deemed uninhabitable and one individual was injured by a shattered glass. The Electricity Authority of Cyprus reported at least 8 smashed or uprooted electric poles, damaged transformers, and loose medium voltage cables. Anticipated costs of the damages are expected to surpass the initial estimation of 2 million euros.

Tenth International Conference on Remote Sensing and Geoinformation of the Environment (RSCy2024), edited by A. Christofe, S. Michaelides, D. Hadjimitsis, C. Danezis, K. Themistocleous, N. Kyriakides, G. Schreier,
Proc. of SPIE Vol. 13212, 132121D · © 2024 SPIE · 0277-786X · doi: 10.1117/12.3037327

Figure 1 Photograph of the tornado on 14 February 2024 approaching Limassol (© Dimitris Georgiou). View toward south.

2. DATA

This study uses meteorological radar data from the Cyprus Department of Meteorology radar network, in synergy with data from the Cyprus Atmospheric Remote Sensing Observatory (CARO) of the Eratosthenes Centre of Excellence. The radar network includes two Plan Position Indicator (PPI) stations, Pafos (PFO) and Larnaca (LCA), whereas CARO, at the time of the tornado occurred, consisted of a Doppler wind-lidar, a ceilometer and a disdrometer. Due to a temporal offset in the ceilometer data, these are not included in this study. Considering the radar network, each radar station is composed of an X-Band Doppler dual-polarization radar that provides continuous information on the estimation of rainfall and hydrometeor classification. Both radars carry out simultaneous horizontal and vertical scanning with spatial resolution of 1º, thus covering the whole extend of Cyprus. On the day of the studied tornado, the radius of LCA was set to 250 km and the radius of PFO to 350 km. Measurements are made with a frequency of approximately 10 minutes. The radars rotate 360° and provide surveillance scans for 8 different elevation angles. Table 1 provides the altitude of each ground-based radar at each elevation angle in Germasogeia, along with details regarding beam blockage. Figure 2 shows the locations of the two ground-based radar stations (LCA and PFO) and CARO on the map. The latter is located in Limassol and at a distance of approximately 10 km from the tornado funnel. The analysis involves damage reports and photographic evidence to capture the trail of the tornado. In the plots presented in the following chapters, the captured trail is marked with "X". The path of the tornado was approximately 4 km long.

Table 1 Radar beam altitudes above Germasogeia area as a function of elevation angle.

Elevation angle [°]	Altitude LCA in Germasogeia [m]	Altitude PFO in Germasogeia [m]	Beam Blockage LCA	Beam Blockage PFO
0.49	600	950	Yes	Partial
1.36	1400	1700	Partial	No
2.22	2170	2450	No	No
3.08	2900	3200	No	No
4.02	3780	4000	No	No
5.67	5300	5500	No	No
9.6	8500	8880	No	No

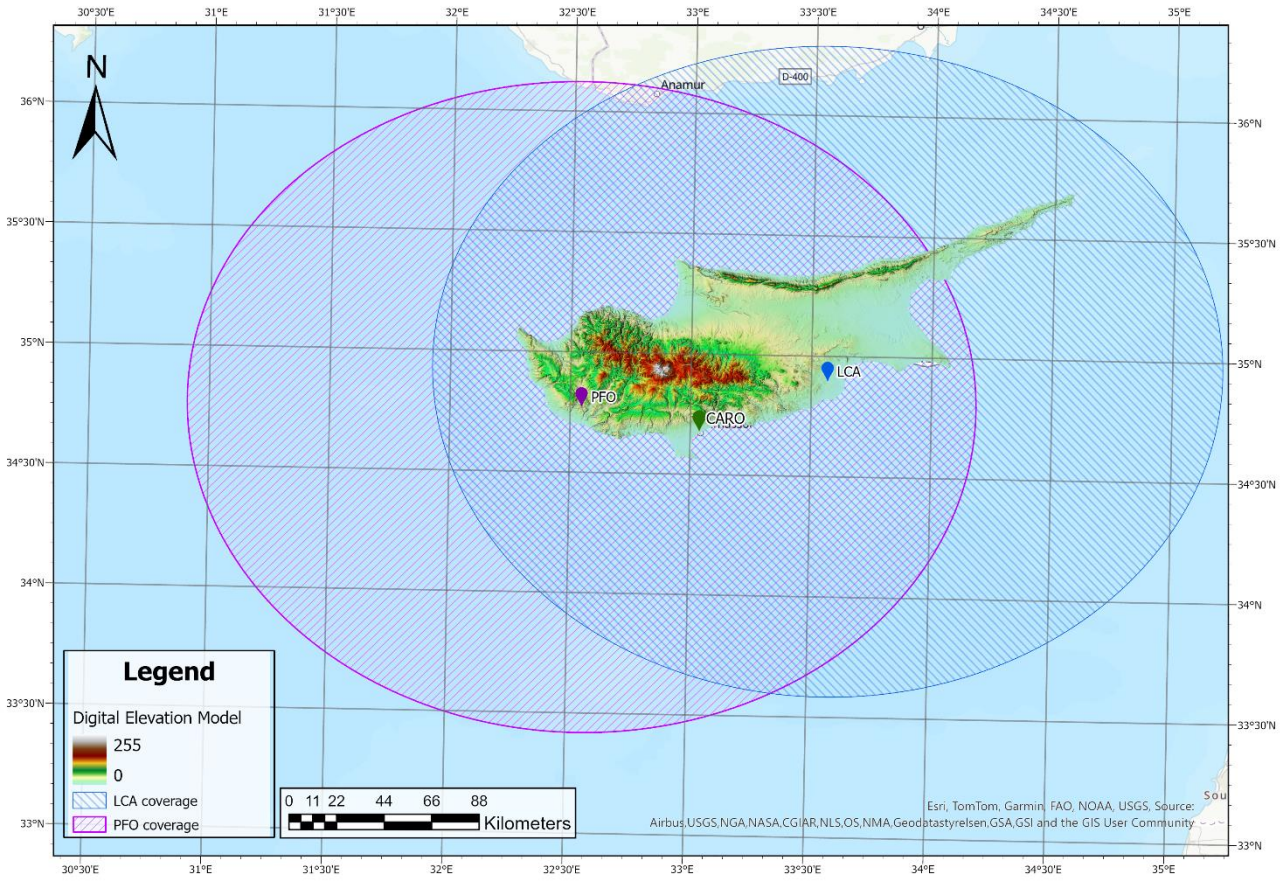

Figure 2 Location of the two ground-based meteorological radars (LCA and PFO) and the CARO site.Figure 3 Location of the two ground-based meteorological radars (LCA and PFO) and the CARO site.

3. PRELIMINARY RESULTS

The wind lidar of CARO recorded vertical winds from -12 to $8\ m/s$ (see Figure 3) and horizontal wind speeds of up to $20\ m/s$ (see Figure 4). Based on the wind speed measurements, the Germasogeia tornado is classified as F0 tornado (gale tornado) in the Fujita Scale [2], whereas based on its type of damage, it could be classified as F1-2 tornado (moderate to significant tornado) in the Fujita Scale. [8] The TORRO (Tornado and Storm Research Organization) International Intensity Scale (T-Scale) is another possible tornado classification. Considering this classification, the Germasogeia tornado could reach a T2-3 scale (moderate to strong tornado) based on the reported damages, but a T0 scale (light tornado) based on the measured wind speed. These deviations are well explained by the fact that CARO is located at a distance of approximately $10\ km$ from the tornado funnel. As shown in Figure 3 and Figure 4, the Doppler wind lidar was able to record the wind travelling towards the station before the tornado and moving away from the station after the tornado. Additionally, a maximum rate of $90\ mm/h$ was measured at the disdrometer of CARO, whereas the whole duration of the rain event at the location of CARO was around $20 min$ (see Figure 5).

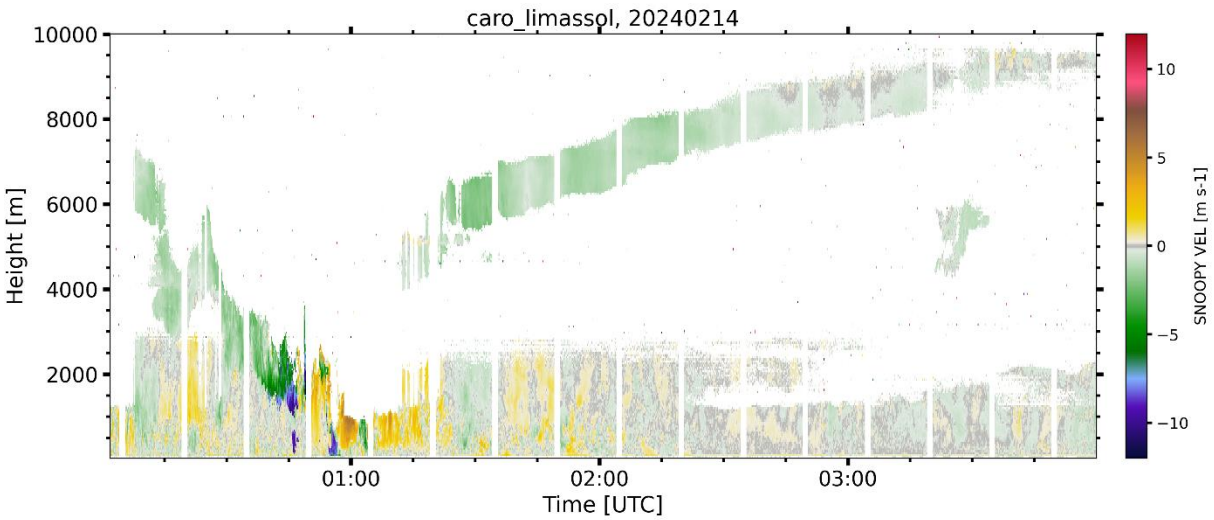

Figure 3 Time-height cross-section of vertical wind velocity as observed by the Doppler lidar at the CARO site on 14 February 2024, 00:00-04:00 UTC.

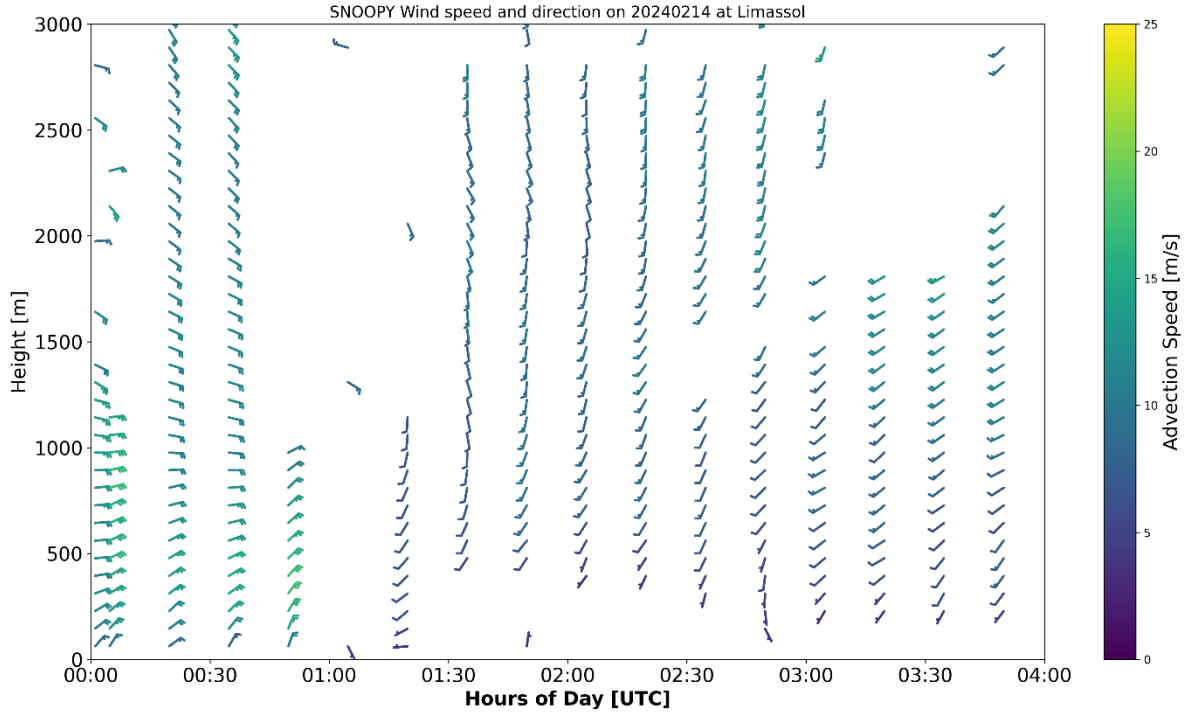

Figure 4 Time-height cross-section of vertical wind velocity as observed by the Doppler lidar at the CARO site on 14 February 2024, 00:00-04:00 UTC.

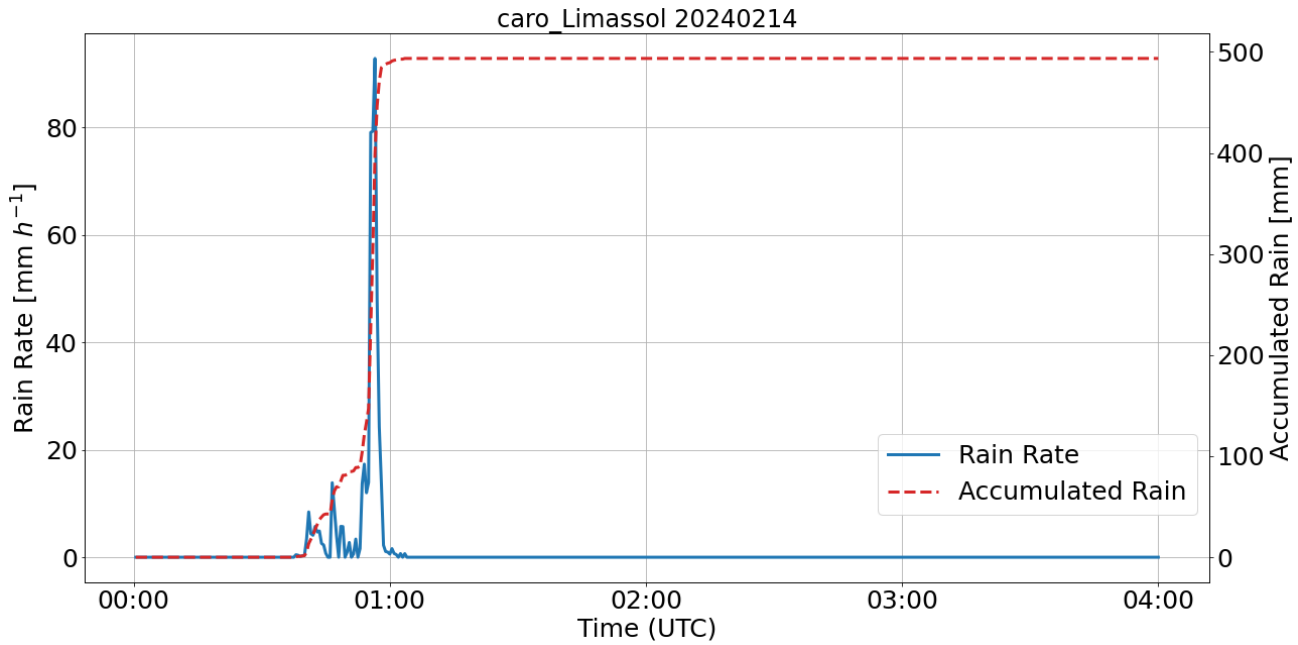

Figure 5 Rain rate [mm h-1] and accumulated rainfall [mm] as retrieved from disdrometer at the CARO site on 14 February 2024, 00:00-04:00 UTC.

Considering the altitude of the beams of both radars at Germasogeia (Table 1) and the maximum height of the Germasogeia tornado, our study examines the horizontal reflectivity and velocity at 0.49°, 1.36° and 2.22° elevation angles (only 2.22° is presented here). As shown in Figure 7 (top, left), PFO ground-radar provides evidence of a hook echo at a proximal distance to the tornado trail. Figure 6 (top, left) shows the presence of a convective cloud with high reflectivity gradients, indicating the possible presence of a cumulonimbus cloud. Considering the radar locations, LCA radar (east of the tornado) was able to better capture the cumulonimbus cloud, which should be found at a higher altitude in relation to the tornado funnel. The velocity couplets shown in Figure 6 (right) and Figure 7 (right) are another significant indication of a tornado as they point to the presence of opposing wind directions, i.e. rotation in the storm. Their strong and tight appearance in the area where the tornado trail was recorded further supports the likelihood of tornado development. Figure 6 (right) and Figure 7 (right) present shear zones in the wider area of central-south Cyprus, indicating areas of strong wind shear.
Velocities are visualized in dark red to dark blue with red gradients indicating inbound winds (moving toward the radar) and blue gradients indicating outbound winds (moving away from the radar). Comparing the LCA records to PFO records, it is worth noting that the presence of opposite colors (red for LCA, where blue for PFO and vice versa) showing similar patterns but in reverse direction. This is because LCA ground-radar is located on the east of the tornado and PFO ground-radar on the west.

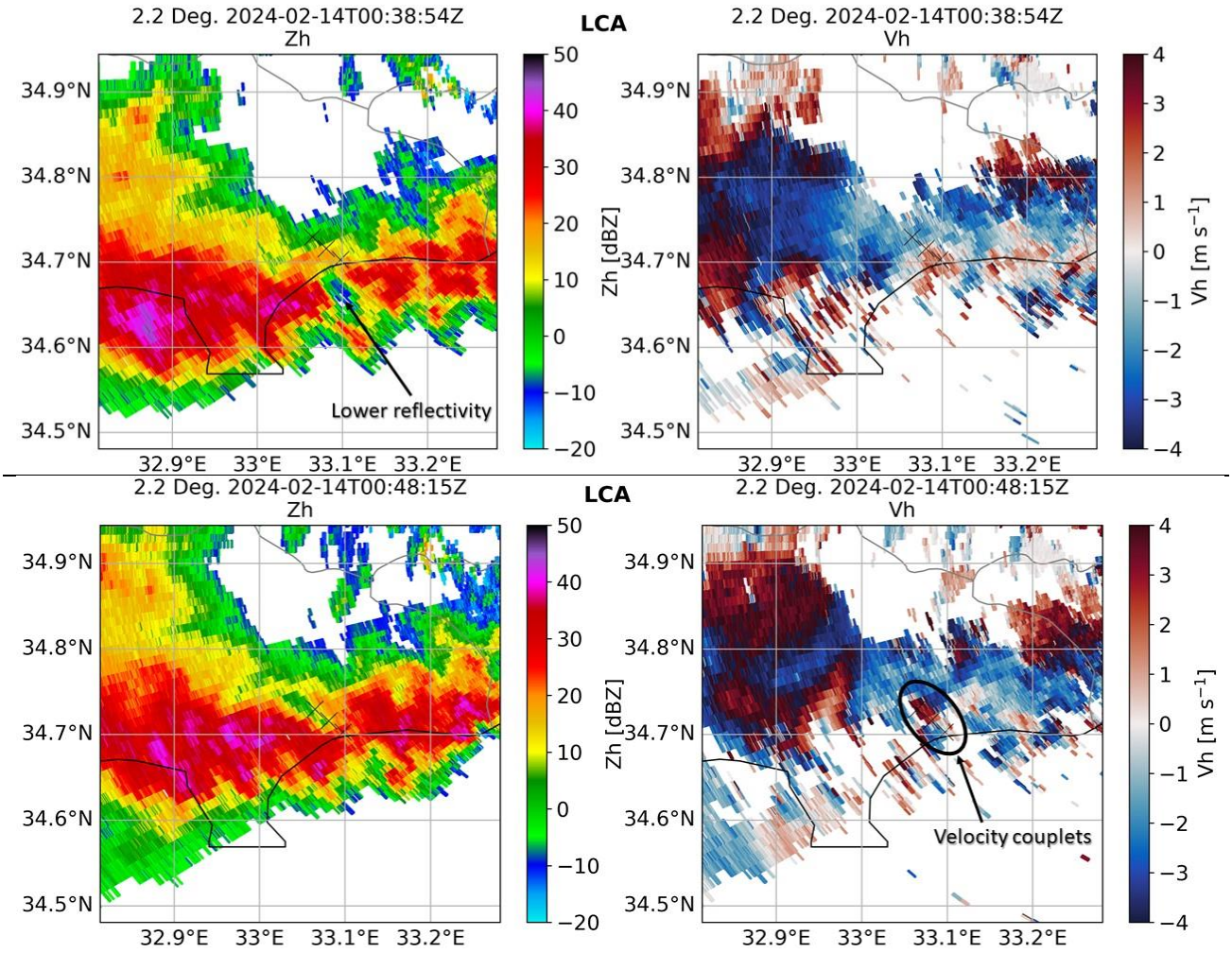

Figure 6 (top) Reflectivity Zh (left) and Velocity Vh (right) of the horizontal polarization plane recorded at LCA ground-radar at 2.2º elevation angle on 14 February 2024, 00:38 UTC, (bottom) Reflectivity Zh (left) and Velocity Vh (right) of the horizontal polarization plane recorded at LCA ground-radar at 2.2º elevation angle on 14 February 2024, 00:48 UTC.

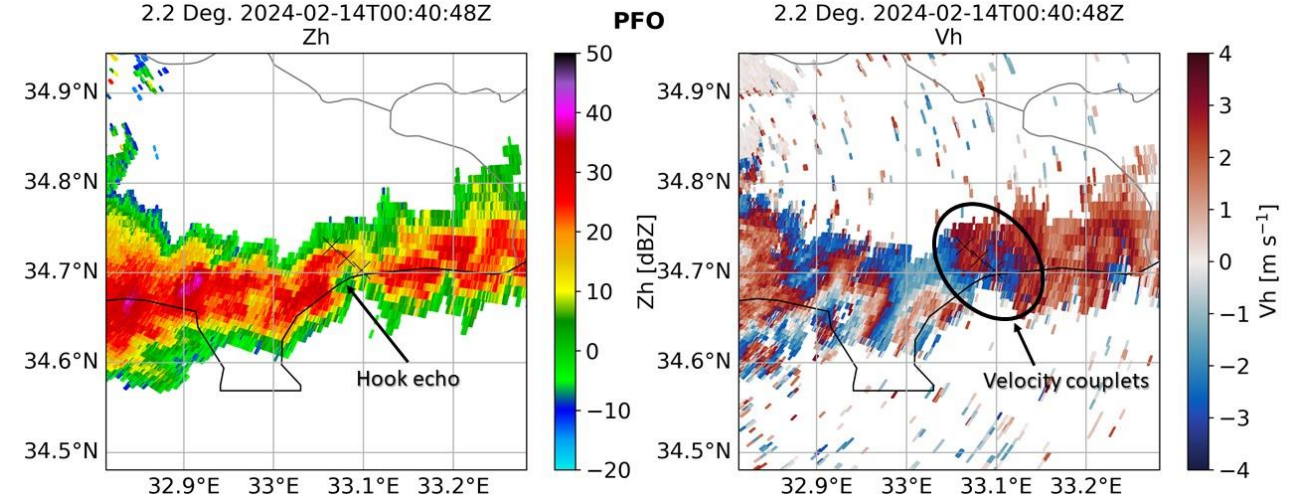

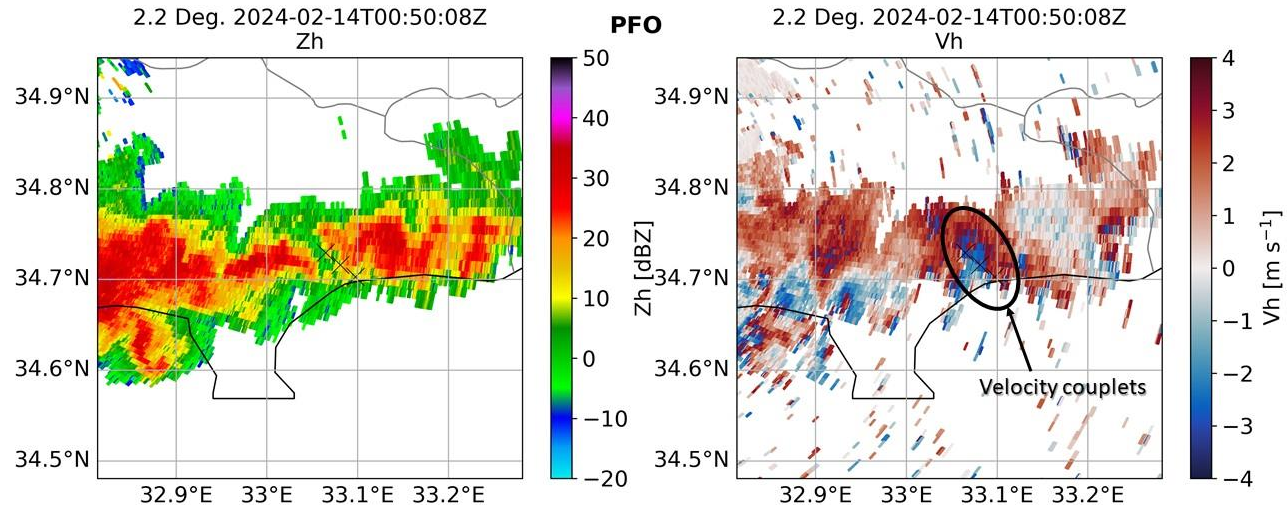

Figure 7 (top) Reflectivity Zh (left) and Velocity Vh (right) of the horizontal polarization plane recorded at PFO ground-radar at 2.2º elevation angle on 14 February 2024, 00:40 UTC, (bottom) Reflectivity Zh (left) and Velocity Vh (right) of the horizontal polarization plane recorded at PFO ground-radar at 2.2º elevation angle on 14 February 2024, 00:50 UTC.

In order to assess the vertical structure of the tornado, we examine the cross section of the radial velocity at the azimuth angle from LCA ground-radar to Germasogeia, which is approximately 50 km away. The azimuth angle from LCA to Germasogeia defines the specific direction at which the cross section is taken. This direction is chosen based on the tornado trail relative to the radar. As presented in Figure 8, velocity couplets are evident at distances between 45 and 55 km from the radar, indicating a tornadic activity within this range. The altitude of the couplets ranges between 3 and 7 km, showing that the rotation extends vertically through approximately 4 km depth. The evidence of velocity couplets at multiple altitudes implies that the rotation extends higher into the storm, indicating a strong and potentially tornadic system.

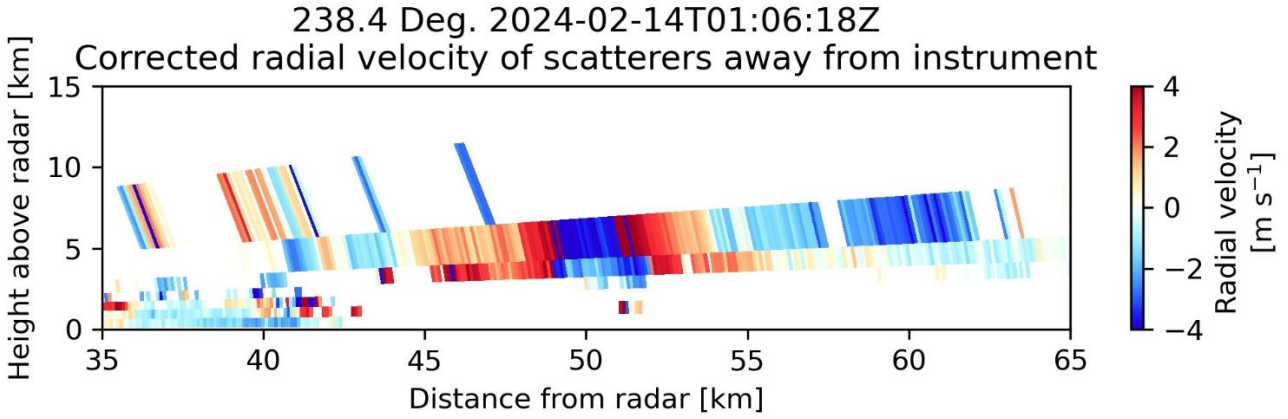

Figure 8 Height-vs-distance cross-section of radial velocity at azimuth angle from LCA ground-radar to Germasogeia, located 50km from radar on 14 February 2024, 01:06 UTC.

4. DISCUSSION

This study presents a preliminary approach in understanding the tornado that occurred in Germasogeia, Cyprus, in the early morning hours of 14 February 2024. The primary aim of our study is to evaluate the suitability of the X-band radar network of Cyprus for detecting and monitoring tornadic activity. Our findings suggest that the current radar setup may present limitations in accurately detecting and monitoring tornadoes, due to velocity folding. Velocity folding occurs when the radar's pulse repetition frequency (PRF) is not sufficient to unambiguously measure high radial velocities that are often associated with tornadoes. In our case, Doppler velocity at both radars ranges between 4 and -4 m/s. The adjustment of

the radar's PRF is necessary to address this limitation. A higher PRF could improve velocity resolution and reduce the unambiguous range, allowing for better accuracy in detecting rotational features., allowing for better accuracy in detecting rotational features. However, balancing the PRF adjustment to avoid range ambiguity is critical to ensure that the radar is still able to distinguish between targets at various distances.

The integration of the meteorological radar data with data recorded at CARO provides a promising approach to enhance our understanding of tornadoes and severe weather phenomena. CARO's atmospheric data can be used to calibrate and validate the radar observations. Additionally, CARO can serve with complementary data such as wind profiles that can provide a better context for the interpretation of the radar measurements. This holistic approach could lead to more precise tornado detection and improved early warning systems, contributing to better public safety and preparedness. In a next step, the information collected about the characteristics of tornado signatures in the precipitation radar network of Cyprus shall be used to screen the 7-years dataset for similar cases. This will provide an estimate of the occurrence frequency of tornado occurrences over Cyprus and will allow to investigate any trends in the occurrence of tornados over the island and of water sprouts near the shore.

ACKNOWLEDGEMENTS

The authors acknowledge the 'EXCELSIOR': ERATOSTHENES: EXcellence Research Centre for Earth Surveillance and Space-Based Monitoring of the Environment H2020 Widespread Teaming project (www.excelsior2020.eu). The 'EXCELSIOR' project has received funding from the European Union's Horizon 2020 research and innovation programme under Grant Agreement No 857510, from the Government of the Republic of Cyprus through the Directorate General for the European Programmes, Coordination and Development and the Cyprus University of Technology.
The authors acknowledge also the Department of Meteorology of the Republic of Cyprus for the provision of the X-band radar data.

REFERENCES

[1] R. Davies-Jones, R. J. Trapp, and H. B. Bluestein, "Tornadoes and Tornadic Storms," in *Severe Convective Storms*, Boston, MA: American Meteorological Society, 2001, pp. 167–221. doi: 10.1007/978-1-935704-06-5_5.

[2] T. T. Fujita, *Proposed characterization of tornadoes and hurricanes by area and intensity*, vol. 91. Satellite and Mesometeorology Research Project, University of Chicago., 1971.

[3] H. B. Bluestein, *Severe Convective Storms and Tornadoes*. Berlin, Heidelberg: Springer Berlin Heidelberg, 2013. doi: 10.1007/978-3-642-05381-8.

[4] P. T. Nastos, K. Karavana Papadimou, and I. T. Matsangouras, "Mediterranean tropical-like cyclones: Impacts and composite daily means and anomalies of synoptic patterns," *Atmos Res*, vol. 208, pp. 156–166, Aug. 2018, doi: 10.1016/j.atmosres.2017.10.023.

[5] T. Toomey, A. Amores, M. Marcos, A. Orfila, and R. Romero, "Coastal Hazards of Tropical-Like Cyclones Over the Mediterranean Sea," *J Geophys Res Oceans*, vol. 127, no. 2, Feb. 2022, doi: 10.1029/2021JC017964.

[6] M. Sioutas, R. Doe, S. Michaelides, M. Christodoulou, and R. Robins, "Meteorological conditions contributing to the development of severe tornadoes in southern Cyprus," *Weather*, vol. 61, no. 1, pp. 10–16, Jan. 2006, doi: 10.1256/wea.268.04.

[7] B. Antonescu, D. M. Schultz, A. Holzer, and P. Groenemeijer, "Tornadoes in Europe: An Underestimated Threat," *Bull Am Meteorol Soc*, vol. 98, no. 4, pp. 713–728, Apr. 2017, doi: 10.1175/BAMS-D-16-0171.1.

[8] P. J. Kirk, "An updated tornado climatology for the UK: 1981-2010," *Weather*, vol. 69, no. 7, pp. 171–175, Jul. 2014, doi: 10.1002/wea.2247.